REPORT DOCUMENTATION PAGE

Form Approved
OMB No. 0704-0188

1. REPORT DATE *(DD-MM-YYYY)*	**2. REPORT TYPE**	**3. DATES COVERED** *(From - To)*
18-12-2009	Technical Paper	

4. TITLE AND SUBTITLE

Accuracy Analysis for Kinetic Modeling of Homogeneous Condensation in Plumes

5a. CONTRACT NUMBER

5b. GRANT NUMBER

5c. PROGRAM ELEMENT NUMBER

6. AUTHOR(S)
Arnaud P. Borner, Zheng Li, and Deborah Levin (Penn State); Ivett A. Leyva (AFRL/RZSA); Ryan Jansen (USC); Sergey Gimelshein and Michael Zeifman (ERC)

5d. PROJECT NUMBER

5e. TASK NUMBER

5f. WORK UNIT NUMBER
23080532

7. PERFORMING ORGANIZATION NAME(S) AND ADDRESS(ES)

Air Force Research Laboratory (AFMC)
AFRL/RZSA
10 E. Saturn Blvd.
Edwards AFB CA 93524-7680

8. PERFORMING ORGANIZATION REPORT NUMBER

AFRL-RZ-ED-TP-2009-443

9. SPONSORING / MONITORING AGENCY NAME(S) AND ADDRESS(ES)

Air Force Research Laboratory (AFMC)
AFRL/RZS
5 Pollux Drive
Edwards AFB CA 93524-7048

10. SPONSOR/MONITOR'S ACRONYM(S)

11. SPONSOR/MONITOR'S NUMBER(S)
AFRL-RZ-ED-TP-2009-443

12. DISTRIBUTION / AVAILABILITY STATEMENT

Approved for public release; distribution unlimited (PA #09519).

13. SUPPLEMENTARY NOTES
For the AIAA Aerospace Sciences Meeting to be held in Orlando, FL, from 4-7 January 2010.

14. ABSTRACT
A model of homogeneneous nucleation based on first principles of the kinetic theory of gases, and developed for the direct simulation Monte Carlo method, is presented. Key parameters of the model, such as the binding energy and the heat capacity as function of cluster size, are given for argon and water. For water, two datasets are used, one based on quantum calculations of heat capacity and binding energy available in the literature, and the other based on the present molecular dynamics computations. The model is analyzed using the thermal bath relaxation problem, and applied to compute the water dimer terminal mole fractions in circular orifice expansion.

15. SUBJECT TERMS

16. SECURITY CLASSIFICATION OF:			**17. LIMITATION OF ABSTRACT**	**18. NUMBER OF PAGES**	**19a. NAME OF RESPONSIBLE PERSON**
					Ivett A. Leyva
a. REPORT	**b. ABSTRACT**	**c. THIS PAGE**	SAR	18	**19b. TELEPHONE NUMBER** *(include area code)*
Unclassified	**Unclassified**	**Unclassified**			N/A

Accuracy Analysis for Kinetic Modeling of Homogeneous Condensation in Plumes

Arnaud P. Borner* and Zheng Li* and Deborah Levin†
Penn State University, State College, PA 16802

Ryan Jansen‡
University of Southern California, Los Angeles, CA 90089

Ingrid Wysong§
Air Force Research Laboratory, Edwards AFB, CA 93524

Sergey Gimelshein¶ and Michael Zeifman‖
ERC, Inc., Edwards AFB, CA 93524

A model of homogeneneous nucleation based on first pronciples of the kinetic theory of gases, and developed for the direct simulation Monte Carlo method, is presented. Key parameters of the model, such as the binding energy and the heat capacity as function of cluster size, are given for argon and water. For water, two datasets are used, one based on quantum calculations of heat capacity and binding energy available in the literature, and the other based on the present molecular dynamics computations. The model is analyzed using the thermal bath relaxation problem, and applied to compute the water dimer teminal mole fractions in circular orifice expansion.

I. Introduction

Two different approaches for modeling the condensation in rapidly expanding plumes have been reported in the literature. The first approach, known as the classical approach, takes its starting point from the classical nucleation theory (CNT) which is based on equilibrium thermodynamics.[1,2] Alternatively, one can treat nucleation as the process of kinetic cluster aggregation.[3] A discussion of the assumptions and difficulties with using CNT for predicting condensation in supersonic expansions can be found in earlier papers.[4–11]

A promising direction in modeling the coupled condensation flow is the use of a kinetic particle simulation method, direct simulation Monte Carlo (DSMC),[12] which is applicable in a wide range of flow regimes from free molecular to near continuum. The DSMC method has been used to study the process of cluster formation and evolution for a number of years.[13–15] However, the gas flow in the earlier studies was uniform, the considered cluster size range was very narrow (up to 25 monomers in a cluster) and the examined reaction types were unrealistically limited to elastic collisions, cluster and monomer sticking to clusters, and evaporation of monomers from clusters. More recently, the DSMC method has been extensively and successfully applied to modeling the processes of cluster formation and evolution in supersonic jets by Levin et al (see, for example, Refs. 9, 16, 17). The model initially was based on CNT, with the new clusters being formed at the critical size. Further work of these authors[18] extended the kinetic dimer formation approach of Ref. 19 (which assumed that a ternary collision always results in a dimer formation), to include molecular dynamic (MD) simulations for obtaining information on the probability of dimer formation in ternary collisions. The work[20] used a temperature-dependent probability of formation of argon dimers. In

*Graduate Student, Aerospace Engineering
†Professor, Aerospace Engineering
‡Undergraduate Student, Astronautical Engineering
§Branch Chief, Propulsion Directorate
¶Consultant

addition, these authors used MD to investigate the kinetics of H_2O dimer formation and showed evidence for a bimolecular mechanism[21] and key predictions were made (using MD) on many needed kinetic parameters for argon[16] and H_2O[22] cluster formation. None of the previous papers as yet have combined the kinetic nucleation mechanism and the kinetic evaporation mechanism together.

A previous paper[23] introduced the present method, where the DSMC approach for modeling of homogeneous nucleation in rapidly expanding plumes is extended to include a number of new features. Most importantly, a kinetic RRK model[24] is implemented to characterize the cluster evaporation rates. Then, an energy dependent collision procedure similar to the recombination reaction model of Ref. 25 is used for the collision complex formation. An empirical parameter is used for the inelastic collision number in the cluster-monomer collisions. For dimers, this parameter is calibrated through the comparison of the computed nucleation rates and equilibrium constants in thermal bath with available theoretical and experimental data for argon and water. The present paper briefly recapitulates the method used and presents a number of updates to the argon and water parameters used. The importance of physically realistic values for parameters is emphasized and new MD results for sample parameter values are presented, along with a discussion of the sensitivity of results to these values. Finally, a new validation case is presented by comparison to published data for H_2O dimer measurements.

II. Numerical Model

The condensation model used in this work is formulated for the DSMC method and is based on first principles of the kinetic theory. The considered processes of cluster nucleation and evolution are modeled at the microscopic level. First principles theory are used to define the main processes of homogeneous condensation, where all collision, nucleation, and evaporation events depend on instantaneous energies of colliding partners, and not cell temperature or other macroscopic quantities. The processes that are included in the model and outlined below are (i) formation of collision complexes through the binary collisions of cluster-forming monomer species and creation of dimers through the collision stabilization of collision complexes, (ii) elastic monomer-cluster collisions that change the translational and internal energies of colliding particles, (iii) inelastic monomer-cluster collisions that result in monomer sticking, (iv) cluster-cluster coalescence, (v) evaporation of monomers from clusters. The description of each of these processes is given below, with all necessary constants and variables specified for two gases considered in this work, argon and water; more detail on the algorithm may be found in Ref. 23.

Dimer Formation One of the important assumptions of the present model is that all pairs of colliding particles create collision complexes. A collision complex is a pair of monomers that have collided, and may have the conditions necessary to form a dimer if struck by a third particle during its lifetime. The collision complex lifetime, t_l, is assumed to be dependent on the type of monomers and their relative collision velocity, with the functional dependence given by the well known Bunker's expression[26]

$$t_l = 1.5\sigma_0\mu^{\frac{1}{2}}\epsilon_0^{\frac{1}{6}}E^{-\frac{2}{3}}, \tag{1}$$

where σ_0 and ϵ_0 are the potential depth and separation distance parameters of the Lennard-Jones (LJ) potential, μ is the reduced mass of the colliding particles, and E is their relative translational energy. The values of σ_0 and ϵ_0 used in this work are 3.2×10^{-10} m and 7.94×10^{-21} J for water, and 3.405×10^{-10} m and 1.654×10^{-21} J for argon. The argon LJ parameters are well known, but H_2O values are roughly estimated by reproducing the known viscosity of water vapor at 273 K and for a small range of temperatures using a LJ potential model.

The process of interaction of collision complexes with surrounding gas particles is modeled using the majorant frequency scheme[27] with the assumption that the collision complex – third particle interactions are governed by the Variable Hard Sphere (VHS) interaction model.[28] The VHS viscosity-temperature exponent ω of a collision complex was assumed to be that of the comprising monomers. For argon atoms, the VHS parameters taken from Ref. 12 were assumed, $d_{ref} = 4.17$ Å and $\omega = 0.81$. For water molecules, $d_{ref} = 6.2$ Å and $\omega = 1$ were assumed, based on reproducing the known viscosity of water vapor at 273 K and for a small range of temperatures using the VHS potential model. Note that the VHS collision diameters are used to compute collision frequency in the cell, while the LJ diameters are only used to compute the diameter and lifetime of a collision-pair complex for purposes of determining the probability of a three-body collision.

For consistency with the collision complex lifetime determination, an expression for the diameter d of the collision complex recommended in Ref. 26 was used,

$$d = 3^{\frac{1}{2}}\sigma_0(\epsilon_0/E)^{\frac{1}{6}}. \tag{2}$$

If there is a physical collision between a collision complex and a third particle, there is a possibility of forming a stable dimer as a result of such a collision. Generally, the probability of the formation of a stable dimer (dimer stabilization) depends on the colliding species and the energies - both translational and internal - of the colliding particles. In this work, constant stabilization probabilities of 0.25 for Ar[18] and 0.7 for H_2O were assumed, which seem reasonable for the range of temperatures under consideration.

Dimer creation through the collisional stabilization of collision complexes is modeled as a two-step process, $L + M \rightarrow (LM)$, $(LM) + K \rightarrow LM + K$. Here, L and M are monomers, (LM) is the collision complex, and K is the third particle.

Reflective collisions of monomers and clusters The collisions between monomers and clusters is one of the key processes that determine the nucleation rate. The reason for this is strong dependence of the evaporation rate on the cluster internal energy. Since the monomers are dominant in the flows considered here, the cluster internal energy is mostly governed by its relaxation through cluster-monomer collisions. In this work, a hard sphere model is assumed for cluster-monomer collisions, with the cluster diameter determined from Eqn. 2 for dimers, and for larger clusters from an empirical correlation used extensively in the past (see, for example, Ref. 8),

$$d = 2 \cdot (A \cdot i^{\frac{1}{3}} + B), \tag{3}$$

where A and B are species-dependent constants, and i is the number of monomers in the cluster. In this work, the values of A and B were 2.3×10^{-10} m and 3.4×10^{-10} m for argon,[16] and 1.9×10^{-10} m and 2.4×10^{-10} m for water.[29]

For the energy transfer between the relative translational and internal modes of the cluster and monomer, the Larsen-Borgnakke model[30] is used, and a parameter Z is introduced that has a meaning of the internal energy relaxation number. The energy transfer between all energy modes of the cluster-monomer pair occurs with a probability Z^{-1}, and an elastic collision with no internal energy exchange occurs with the additional probability $1-Z^{-1}$. For argon, temperature dependent values of $Z(T)$ were used, obtained through the linear interpolation between the values given in Table 1. Similar to temperature dependent collision numbers for rotational and vibrational relaxation of molecules widely used in the DSMC method, T was the cell-based translational temperature. Such a temperature dependence allows good agreement of the DSMC rates for dimer nucleation and dissociation with rates available in the literature. For water condensation, a constant value of $Z = 10$ was used, which corresponds to that for rotational and vibrational relaxation of water molecules at romm temperature obtained in molecular dynamics studies.[31,32]

T, K	0.0	100.0	200.0	300.0	400.0	500.0
Z^{-1}	0.25	0.13	0.08	0.06	0.046	0.04

Table 1. Inelastic collision number as function of temperature for argon.

Sticking of monomers and clusters When a monomer collides with a cluster, sticking of the monomer to a cluster surface is possible, in addition to a reflective collision described in the previous section. For small clusters, monomer sticking is the main process that governs the evolution of the droplet size distribution.[33] For water molecules, an empirical dependence of the sticking probability on the species radius and mass, given in Ref. 34, is used. This dependence reduces to

$$\epsilon = \frac{d_n^2}{(d_n + d_1)^2}\left(\frac{m_n}{m_n + m_1}\right)^{\frac{1}{2}}, \tag{4}$$

where indices n and 1 refer to the cluster and monomer, respectively.

For argon, the sticking probability of monomers on clusters given in Table 2 is used

Similar to monomer-cluster collisions, the outcome for cluster-cluster collisions is assumed to be either coalescence or elastic interaction. The probability of sticking was assumed to be unity both for argon and water in cluster-cluster collisions.

Cluster size	2	3	4	5	6	7	8	9	10	11	12	13	14	15
Probability	0.06	0.075	0.1	0.16	0.3	0.5	0.67	0.75	0.8	0.833	0.857	0.876	0.891	0.9

Table 2. Sticking probability as function of cluster size for argon.

CLUSTER EVAPORATION Following Ref. 35, RRK theory is used to model the evaporation process. The evaporation rate k_e is calculated as

$$k_e = \nu N_s \left(\frac{E_{int} - E_b}{E_{int}} \right)^{3n-7} \tag{5}$$

Here, n is the number of monomers in the cluster, ν is the vibration frequency, N_s is the number of surface atoms, and E_{int} is the cluster internal energy. For dimers, the exponent $3n-7$ is replaced with 1. The number of surface atoms is n for $N < 5$, $n-1$ for $4 < n < 7$, and $(36\pi)^{1/3}(n^{1/3}-1)^2$ for $n > 6$. The vibration frequency was taken to be 2.68×10^{12} s^{-1} for water clusters,[36] and 10^{12} s^{-1} for argon clusters.[36]

It is important to use reasonable values for the evaporation energy of a monomer off a cluster, as well as the number of cluster internal degrees of freedom, as a function of cluster size. In this work, two data sets were used for water heat capacities and binding energies. The first one is described in this section; hereafter it is referred to as Dataset 1. The second data set is based on water dimer and trimer heat capacities calculated with the approach presented in the next section.

The evaporation energy of a monomer from an n-cluster is given by $E_b(n) - E_b(n-1)$, where E_b is the binding (evaporation) energy of the n-cluster. The E_b values for water clusters (Ref. 37) were taken from Ref. 38 for $n = 2-8$ (and subtracting the zero-point energies, taken from ref Ref. 39), and using smoothed values from Refs. 40, 41 for $n = 9-13$. These baseline values of the evaporation energy for water clusters are used in (Dataset 1). Evaporation energies were taken from Ref. 42 for argon clusters. The number of cluster internal degrees of freedom is calculated from the expression for the average internal energy $\langle E \rangle$ of a cluster of a size n

$$\langle E \rangle = \frac{\xi^{int}}{2} kT = nC_v T - \frac{3}{2} kT$$

as

$$\xi^{int} = n\frac{2C_v}{k} - 3$$

where C_v is the cluster heat capacity. For water, the values of C_v where adapted from Refs. 43, 44 (Dataset 1), while for argon, they where assumed to approximate an expression $\xi^{int} = 2(3n-\eta) + \epsilon$, where $\eta = 5$ and $\epsilon = 2$ for $n = 2$ and $\eta = 6$ and $\epsilon = 3$ otherwise.[45] Note that for water dimers, the number of degrees of freedom was assumed t be a function of internal energy (or effective temperature), decreasing linearly from its listed value at 200 K to 3 at 0 K. Both the heat capacity and evaporation energies are listed in Table 3. For the cluster sizes larger than given below, the values for the maximum listed sizes are used.

The first-principles condensation model described here was implemented in the DSMC code SMILE.[46]

III. Calculation of Water Dimer and Trimer Heat Capacities

Water clusters have been subject to several experimental and theoretical studies. Tsai and Jordan[47,48] studied the phase transition of water octomers. The single histogram method[49] and jump-walking procedure[50] were used in those studies. The former allows one to perform a single Monte Carlo simulation at some specified temperature and extrapolate the results to other nearby temperatures.[51] The latter carries out calculations for a range of temperature, starting at a 'high' temperature and stepping to lower temperatures. The initial calculation at temperature T_1 is carried out using standard Metropolis sampling. Then, at each successive temperature T_i, sampling is done by occasionnally jumping to a distribution generated at the preceding temperature T_{i-1}. TIP3P[52] and TIP4P[53] potentials were used in those Monte Carlo simulations. Plots of the potential energy and heat capacity as a function of the temperature were generated. A Molecular Dynamics study of $(H_2O)_{n=2,3,4,6,8}$ clusters was conducted by Guvenc and Anderson.[54] Melting temperature was plotted as a function of cluster size, and the ones for the dimer and the tetramer closely ressemble the bulk melting temperature, while those for the other sizes were considerably lower. Pedulla and Jordan[55] studied the melting behavior of $(H_2O)_6$ and $(H_2O)_8$ water clusters. The location and sharpness of the melting transition were investigated for different potential models. It was found that the position

Cluster size	H_2O E_b, J	H_2O C_v, J/K	Ar E_b, J	Ar C_v, J/K
2	2.455E-20	3.726E-23	1.98E-21	2.41E-23
3	5.352E-20	4.830E-23	3.96E-21	2.76E-23
4	6.325E-20	5.748E-23	5.94E-21	3.10E-23
5	4.726E-20	6.555E-23	6.08E-21	3.31E-23
6	4.587E-20	7.245E-23	6.89E-21	3.44E-23
7	5.560E-20	7.817E-23	7.49E-21	3.54E-23
8	6.950E-20	8.277E-23	6.36E-21	3.62E-23
9	5.560E-20	8.648E-23	8.29E-21	3.68E-23
10	5.699E-20	8.970E-23	8.25E-21	3.72E-23
11	5.838E-20	9.227E-23	8.27E-21	3.76E-23
12	5.977E-20	9.467E-23	9.86E-21	3.79E-23
13	6.116E-20	9.654E-23	12.2E-21	3.82E-23

Table 3. The water and argon cluster heat capacities and evaporation energies per monomer.

of the peak in the heat capacity curve was quite sensitive to the specific model potential. The results obtained when using canonical and microcanical ensembles for Monte Carlo simulations applied to study water tetramer and octamer were compared.[56] A TIP5P potential model[57] was implemented. The microcanonical heat capacity curve was found to have a sharper peak than the canonical one, but the locations of the peaks were found to be the same. The phase change of water octamer clusters was investigated[58] by performing Molecular Dynamics simulations with a SPC/F_2 potential model.[59] The phase transition is found to occur around 125 K.

A. Simple Point Charge Water Model

The interactions among water molecules are dominated by dipole interactions. One effective way to describe such interactions is to consider three point charges, one on each atom. In the SPC model,[60] the water molecule is modeled to have three centers of concentrated charge: a positive charge on each of the two H atoms and a negative charge on the O atom. The assumption that there are point charges is an approximation that leads to an incorrect value for the permanent dipole moment of the water molecule. To correct this, the H–O–H bond angle is changed from the true value of 104.45 to 109.47 degrees in the SPC model. As a consequence of the charge concentration and the widened V–shaped bond angle, the permanent dipole moment of the SPC-model water molecule has a value close to that measured in experiment of 1.85 D.

In summary, the SPC model consists of a triangular water model with an OH distance of 1 Å (compared to the true bond length of 0.9584 Å), with point charges on the oxygen and hydrogen positions of -0.82 and +0.41 e (electronic charge units), respectively. The corresponding potential is a combination of Lennard-Jones interactions between the oxygen atoms of each water molecule,

$$U^{\mathrm{LJ}}(r) = 4\epsilon^{\mathrm{LJ}}\left[\left(\frac{\sigma^{\mathrm{LJ}}}{r}\right)^{12} - \left(\frac{\sigma^{\mathrm{LJ}}}{r}\right)^{6}\right] \tag{6}$$

with the parameters of $\sigma^{\mathrm{LJ}} = 3.166$ Å, $\epsilon^{\mathrm{LJ}} = 0.65$ kJ/mol and the Coulomb potential between all the atoms,

$$U_{ij}^{\mathrm{Coulomb}}(r_{ij}) = \frac{q_i q_j}{4\pi\epsilon_0 r_{ij}} \tag{7}$$

where q_i, q_j are the charges of O or H atoms and ϵ_0 is the permittivity of free space.[22]

B. Monte Carlo Canonical Ensemble Simulation

For cluster-monomer interactions, the initial separations between molecules inside a cluster and their velocities have a great effect on the calculation of the potential energy. Therefore a high number of initial configurations (between 400 and 4000) is chosen to reduce the statistical error. In order to prepare the

initial position configurations for clusters, the Monte Carlo canonical ensemble simulation method is used.[61] In this approach, a sphere domain is setup with a known radius, R_i, which depends on the cluster size, i. The initial molecules (for example, 2 molecules for a dimer) then are randomly put in the spherical domain and one of the molecules is moved a small distance from its original point as shown in Figure 1. The system potential energy is calculated based on the SPC model and designated as, U_{o}. The system is allowed to evolve for a large number of steps and for each time step, one of the molecules is randomly moved in the sphere and the new energy U_{n} is calculated. The move is accepted with probability,

$$P_a = \min(1, \exp(-[U_{\mathrm{n}} - U_{\mathrm{o}}))/kT) \tag{8}$$

where T is the temperature and k is Boltzmann's constant. After 10,000 steps, the system is assumed to be in equilibrium and an accepted configuration is recorded every 100 steps. The so-called 'baby steps' ensure a higher number of configurations are accepted. The molecule is also rotated with a small angle change compared to the angle at the previous step as shown on Figure 2. The system is run for 1,000,000 timesteps. Six independents Monte Carlo cycles were computed at every temperature.

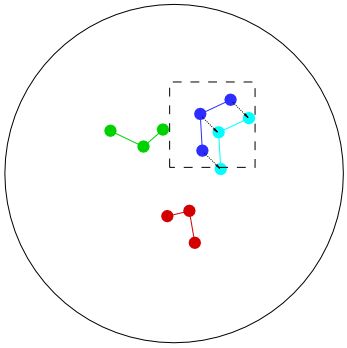

Figure 1. Water trimer plot showing the outside boundary sphere (radius = 2.8 Å) and an imaginary cube (length = 0.28 Å) inside which 'baby translations' are allowed.

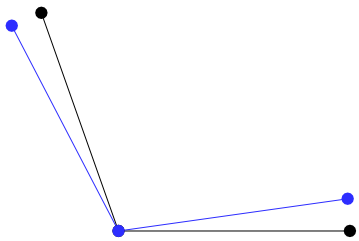

Figure 2. The water molecule is rotated through a small angle equal to 0.2π.

C. Potential Energy and Heat Capacity Calculation

The potential energy of the system is calculated by summing the SPC potential due to each molecule in the cluster. Then it is normalized by dividing by the number of molecules in the cluster. The constant volume

heat capacity is computed as

$$C_v = \frac{< U^2 > - < U >^2}{3RT^2} + 3R \tag{9}$$

where R is the ideal gas constant. The standard deviations are based on the 6 independent cycles at each temperature.

D. Results of Molecular Dynamics Calculations

Figure 3 shows the potential energy of a water molecule in a dimer as a function of the ensemble temperature. It can be seen that the potential energy increases with the temperaure, almost with a linear trend. Figure 4 shows the constant volume heat capacity as a function of the temperature. Even though the value of C_v fluctuates a lot with temperature, the general trend that can be seen from this plot is that there is a peak around 220 K. This point where the heat capacity reaches reaches its maximum is known as the melting point. This value is relatively close to the one found by Guvenc and Anderson,[54] 275 K. The heat capacity fluctuates around 10 cal/mol/K, while the one for liquid water is about 18 cal/mol/K at 300 K.

The results for the water trimer are shown in Figures 5 and 6. The same linear trend as for the dimer can be seen again in the case of the trimer. The values of the potential energy are about double those of the dimer. The trend for the heat capacity of the trimer is also similar to the one of the dimer. The heat capacity fluctuates around 10 cal/mol/K and seem to have a melting point around 240 K.

In this work, the dimer and trimer heat capacities of 10.2 cal/mol/K and 12 cal/mol/K were used in Dataset 2. The binding energy of $3e-23$ J was used for dimer in order to reproduce theoretical equilibrium constants (see below); for larger clusters, the binding values from Table 3 were taken.

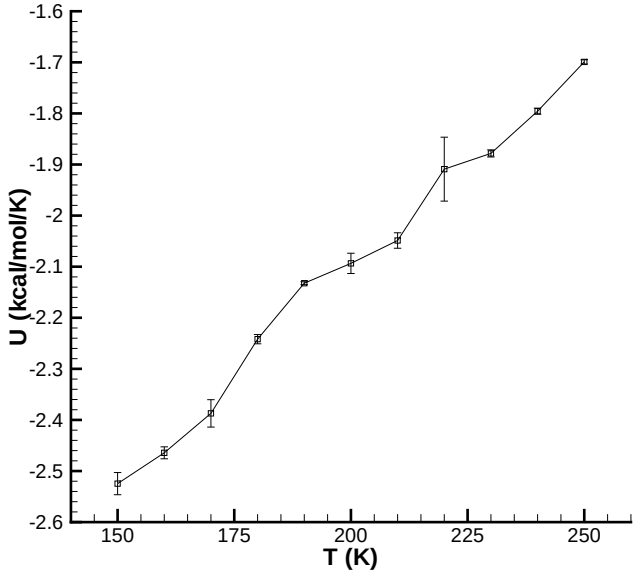

Figure 3. Potential energy of a water molecule inside a dimer for different cluster temperatures. The standard deviations are computed from six 2-million cycles of calculations.

IV. Thermal bath relaxation

Inelastic cross sections for monomer-monomer and monomer-cluster collision processes are necessary for detailed validation of a kinetic condensation model. These cross sections, generally functions of the energy states, both translational and internal, of pre- and post-collisional particles, are not available for most gas and temperature conditions of interest. Contrary to the energy dependent cross section, the integral temperature dependent rates for such collisions at conditions close to equilibrium are available in the literature. Therefore,

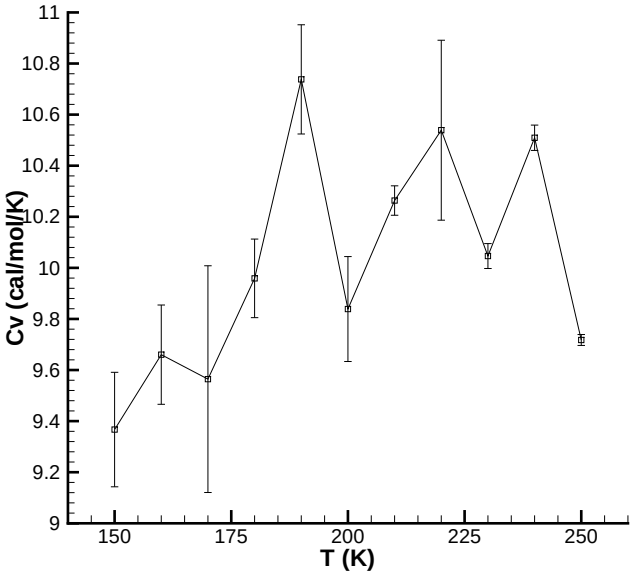

Figure 4. Constant volume heat capacity of a water molecule inside a dimer for different cluster temperatures (heat capacity per molecule).

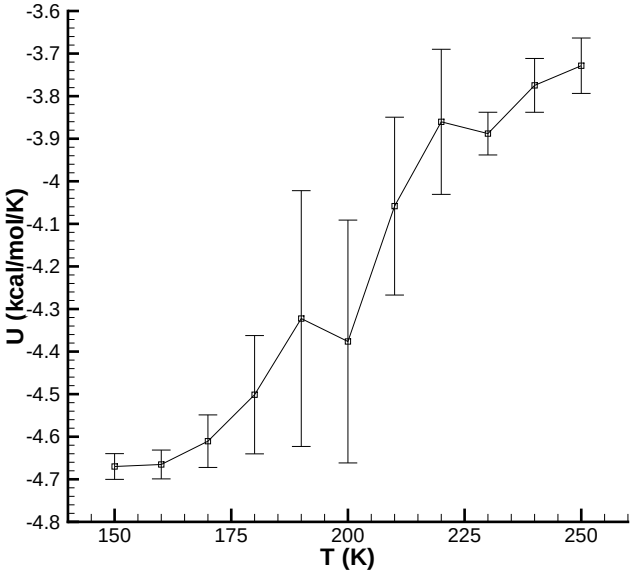

Figure 5. Potential energy of a water molecule inside a trimer for different cluster temperatures. The standard deviations are computed from six 1-million cycles calculations.

one of the key indicators of the accuracy and reliability of a condensation model is its ability to produce realistic rates of evaporation and nucleation at equilibrium. Although matching the rates generally does not guarantee correct behavior in nonequilibrium, it still is a necessary condition for a model to satisfy.

In this work, thermal bath relaxation of pure argon and pure water are examined at different temperature conditions, and the dimer formation rates for argon and equilibrium constants for the formation of dimers

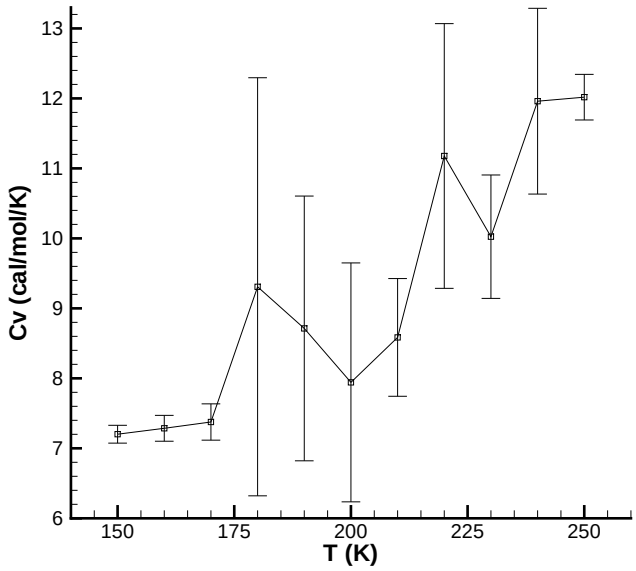

Figure 6. Constant volume heat capacity of a water molecule inside a trimer for different cluster temperatures (heat capacity per molecule).

in argon and water are calculated and compared to the published results.[43,62–65] In all thermal bath results, one million simulated particles were used, and the run proceeded until the steady state is reached, after which the results were sampled for 20 thousand timesteps. The number density was 5×10^{23} molec/m^3 for argon and 2×10^{23} molec/m^3 for water. The timestep of 2.5×10^{-11} s was selected so that the number of collisions per molecule is much smaller than unity, and the results are independent on the timestep.

The computed dimer formation rates k_{rec} for argon are presented in Fig. 7 and compared with the stable dimer formation rate of Ref. 62, where they were calculated using classical trajectories, and the following expression was proposed,

$$k_{rec} = 10.15 T^{-0.278} \exp\{-0.0031T\}.$$

Generally, the present dimer formation rates are in good agreement with the classical trajectory calculations, with the maximum difference approaching 20% for higher temperatures. Note that the computed rate has somewhat different slope than that of Eqn. IV. A number of factors could be affecting the slope, among them are the energy dependence of the stabilization probability and dimer heat capacity, which were not included in the present model.

The computed equilibrium constant, K_{eq}, that is the ratio of the dimer dissociation to the dimer formation rate, is given in Fig. 8. It is compared to the theoretical results of Ref. 63, where a number of approximate classical and quantum methods are compared with exact numerical calculations, and also experimental results of Ref. 64 and theoretical results of Ref. 65. Note that while the results for different models and interaction potentials where found to be widely different in Ref. 63, there was a good agreement between analogous quantum and classical calculations. Figure 8 shows that for the entire temperature range there is an excellent agreement between the present model and the theoretical and experimental values. The reasona for such a good agreement is the appropriate selection of the temperature dependence of the inalastic collision number Z.

This parameter, which s in effect the inverse probability of the energy transfer between the internal modes of a dimer and the translational modes in dimer-monomer collisions, was found to be an important factor that influences the magnitude of the equilibrium constant K_{eq}. This may be explained as follows. The dimers are formed after three-body collisions, and typically have internal energies smaller than the evaporation energy after those collisions. In argon, the evaporation energy for a dimer is relatively small compared to the typical total collision energy for all temperatures under consideration ($E_b/k \approx 140$ K). That means that most of the dimers will have their internal energy in excess of the evaporation energy just after one or two collisions

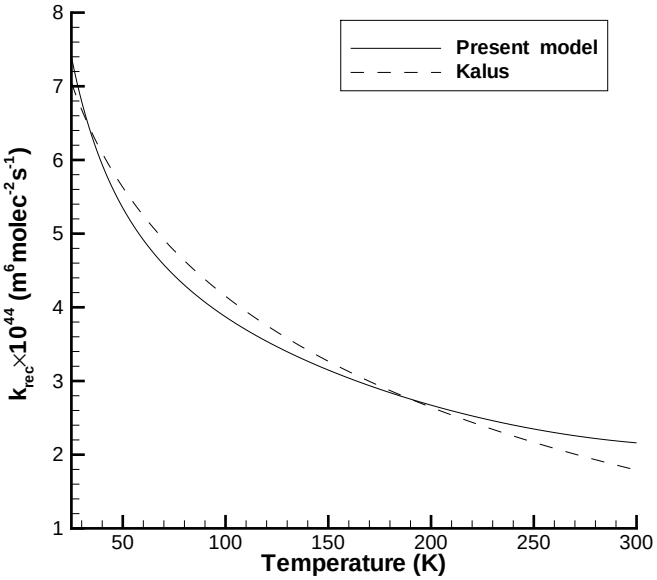

Figure 7. Argon dimer formation rate as a function of gas temperature.

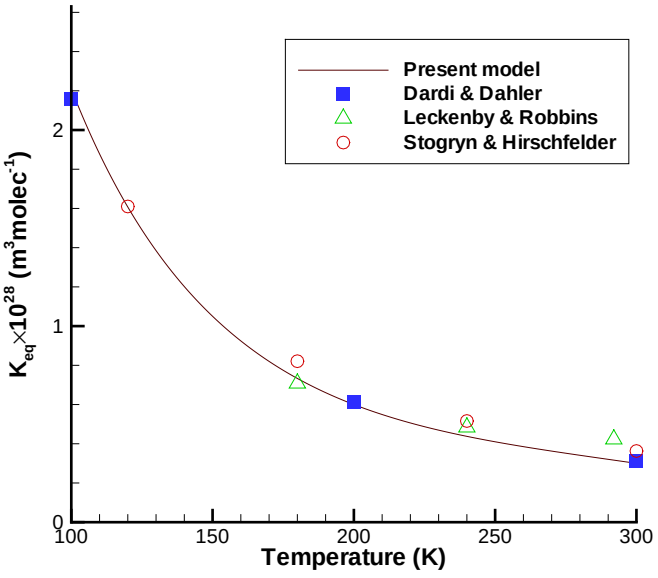

Figure 8. Argon dimer formation equilibrium constant as a function of gas temperature.

with monomers. The lifetime of the dimers whose internal energy is larger than the evaporation energy is very short, on the order of a picosecond. This results in the dimer-monomer energy transfer being the main process that leads to quick dimer dissociation. Note that the value of Z has negligible impact on the dimer formation rates, and only the evaporation rates are affected. As a result, in the range of temperatures considered in this work, the equilibrium constant for argon was found to be nearly proportional to Z^{-1}.

The Z dependence of the equilibrium constant is weaker for water molecule condensation. In this case, the evaporation energy of a dimer is much larger than the translational energy of colliding molecules and dimers (the reduced evaporation energy $E_b/k \approx 3,500$ K, compared to gas temperatures on the order of 300 K). The high value of the evaporation energy results in longer lifetimes of dimers, since much more collisions are necessary to transfer enough energy from the translational modes to the internal modes of a dimer. The dependence of K_{eq} on Z is therefore much weaker for water than for argon. In a 250 K thermal bath, K_{eq} was found to decreases by only about a factor of two when Z decreases from 10 to 1.

Comparison of the equilibrium constant obtained with the present model and two different datasets, with the theoretical results of Refs. 43, 66, where a flexible potential energy surface fitted to spectroscopical data was used, is shown in Fig. 9. Note that there are a number of theoretical predictions of the equilibrium rate of water dimerization, and they differ by at least a factor of three in the range of temperatures considered in this work. Reference 43 was chosen for comparison as the most sophisticated and one of the most recent ones. The results for Dataset 1 show that the calculated equilirbium constant agrees well with the theorecal prediction for temperatures 160 K and 250 K, the range that is expected to be very important in terms of dimer formation and nucleation in plume expansions. The calculated values for higher temperatures significantly overpredict the theoretical curve. For dataset 2, the results are close to Refs. 43, 66 for temperatures between 200 K and 350 K. For lower temperatures, the calculated values are noticeably smaller. The difference between Satasets 1 and 2 is within a factor of two for the entire range of temperatures under consideration, which indicates that the change in the binding energy and heat capacity, that are assumed to be temperature independent, do not significantly change the slope of the equilibrium constant decreasing with increasing temperature. This general trend of weaker slope may be related to a number of factors, such as temperature dependence of actual heat capacity and evaporation energy, as well as the approximate after-reaction energy redistribution used in this work (recall that the Larsen-Borgnakke model was used for the energy redistribution).

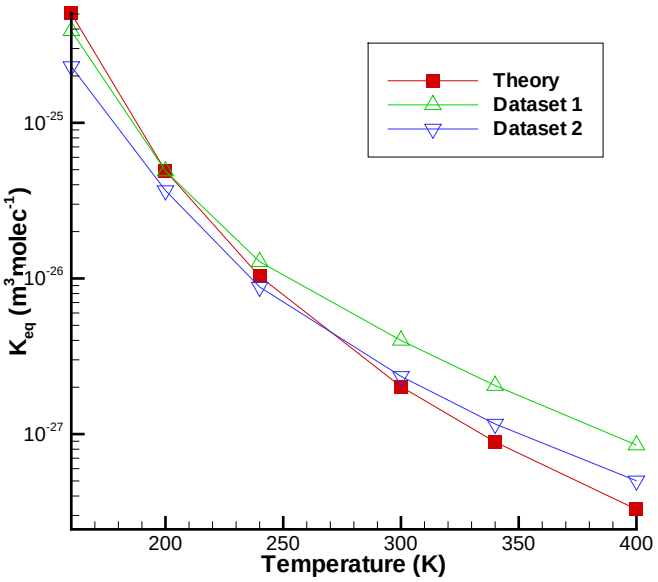

Figure 9. Water equilibrium constant as a function of gas temperature.

V. Orifice Expansion Flow

An experimental study[67] of dimer formation in supersonic water vapor molecular beams expanding from a circular orifice is chosen as the basis for comparison and analysis of the present algorithm and parameters of the numerical model. The flow of water vapor through a 123 /mum diameter orifice is modeled for a chamber pressure ranging from 30 torr to 300 torr, and two reservoir temperatures of 373 K and 493 K. In the DSMC simulations, the subsonic boundary conditions were set far enough from the orifice plane to avoid any impact of their location. Fully diffuse accommodation on the wall was assumed. To avoid slow convergence associated with the subsonic part of the domain, the calculations included to steps. First, the flow was calculated in the free molecular regime. Then, the simulated molecules from the first step wer utilized as the initial condition for the second, high pressure, step. The typical numbers of simulated molecules and collision cells were 20 million and 2 million, respectively. Dataset 1 is used in all presented results except those explicitely indicated.

The gas temperature fields and the cluster number density fields (all cluster sizes included) are presented in Fig. 10 for the smallest and highest pressures under consideration. While the gas temperature fields are qualitatively similar, there is some quantitative difference between 30 torr and 300 torr cases that is expected to be substantial in terms of vapor condensation. In the near field of the orifice, the coreflow temperatures are significantly lower for the low pressure case. It is closely related to the gas mean free path in this region. As density decreases sharply in the expansion, there is relatively few collisions in the plume for the 30 torr case. This results in larger deflection from the symmetry axis, and as a result lower gas temperatures in the coreflow. Further downstream, larger collision frequency results in lower freezing temperatures; at distances larger than 1 mm from the orifice plane the gas temperature at 300 torr is lower than at 30 torr. For both pressures, there is a significant number of clusters in the plenum. Generally, their number corresponds to the equilibrium constant at a given temperature and density; it is two orders of magnitude larger for the higher pressure case. The descrease in the plume is more pronounced for this case.

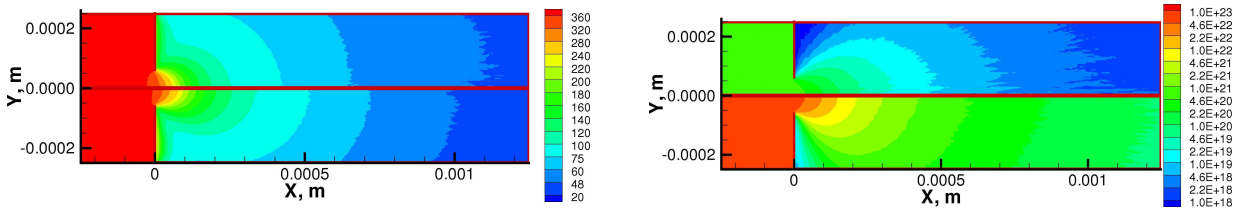

Figure 10. Impact of chamber pressure on gas translational temperature (K), left, and cluster number density (m^{-3}), right. Top halves, $p_0 = 30$ torr, bottom halves, $p_0 = 300$ torr.

This decrease is illustrated in Fig. 11, where the cluster mole fraction normalized by its chamber value is presented along with the water vapor temperature for two plenum pressures. It is clearly seen that the relative increase in the cluster mole fraction is more significant for the lower pressure. The reason for this is that even though the relative gas density in the coreflow is higher for 300 torr, which results in more clusters produced, it is not compensated by significantly lower temperatures in the expansion region for this case. For example, 100 /mum downstream from the orifice plane the temperature for 300 torr case is about 35K lower, which translates to over five times lower dimer equilibrium constant. Most of the condensation occurs at temperatures between 300 K and 150 K. Note that at about 200 /mum from the orifice plane the cluster mole reaches a plateau, at which point any further increase in the mole fraction along the symmetry axis is primarily due to gasdynamic reasons (heavier particles tend to stay in the coreflow), and not as much due to the condensation-evaporation mechanism. For a higher stagnation temperature of 493 K, the dimer mole fraction start to increase at about 450 K, and increases until the gas is colled down to about 150 K, at which point further increase is hampered by relatively low collision frequencies.

While the knowledge of total cluster mole fractions may be important in many cases and applications, it is also important to know the size distribution of these clusters. Generally, it may change from nearly Gaussian at low pressures to bi-model at higher pressures.[33] The terminal size distribution of water clusters for the cases under consideration is shown in Fig. 12. Wvwn though it is difficult to draw any conclusions for the two smaller pressures, the size distribution is certainly non-Gaussian for the two larger pressures. The upper levels are clearly underpopulated as compared to a Boltzmann-like equilibrium distribution. The reason maybe fast cooling and simultaneous increase in the gas mean free path in the expanding plume

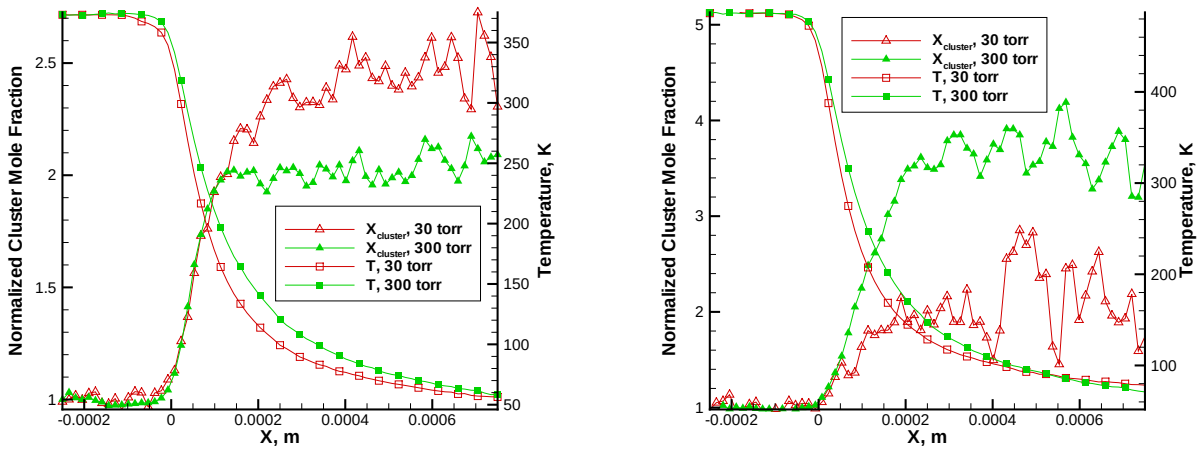

Figure 11. Gas temperature and cluster mole fraction profiles along the orifice axis for a stagnation temperature of 373 K (left) and 493 K (right).

flow, where there are not enough collisions to produce significant number of clusters larger than 4-mers. Nevertheless, note that at 300 torr the relative population of dimers is less than 50%, the rest is larger clusters. The dimer population increases to over 60% for 200 torr and to about 85% for 100 torr. For 493 K cases (not shown here), the relative population of of trimers is 9% for 300 torr, 2.5% for 200 torr, and less than 1% for 100 torr. The number of larger clusters is negligible for this temperature.

Comparison of the numerical results for the terminal mole fraction of dimers near the symmetry axis with experimental results[67] is presented in Fig. 13 (right) for two considered stagnation temperatures. For both temperatures, there is a reasonable agreement for lower pressures where the dimers comprise well over 90% od the total number of clusters. For higher pressures, where the important processes include not only the dimer formation rate, but also cluster coalescence and monomer sticking, the computational results significantly underpredict the data. Additional computations conducted for 373 K with the coalescence probability reduced from the baseline of 1 to 0.2, show the terminal dimer mole fraction increase to 0.02 at 200 torr and 0.021 at 300 torr. Although it still underpredicts the data, it is over a factor of two higher than the baseline values. The calculations were also performed for Dataset 1 (not shown here); the results are generally about 25% lower than for Dataset 2. For example, for 100 torr at 373 K it is 0.006 instead of 0.0083 for Dataset 2. This was expected since for Dataset 1 the dimer formation equilirbium constant is significantly higher at low temperatures. There may be a number of possible reasons for the difference between the experimental and numerical data which root both in computational and measurement procedures and uncertainties. Practically all parameters used in the present model and listed in the previous section have significant error bars. Experimental data also have error bars related to the assumed cross sections, intrusions introduced by the ionization precedure. The actual geometry of the orifice, such as the orifice thickness, as well as orifice surface temperature distribution, are also unclear. The present model better captures the decrease in the mole fraction due to the stagnation temperature increase than the model[10] (see Fig. 13, left), but again, it is less pronounced than in the experiment.

VI. Conclusions

The homogeneous condensation model for the DSMC method is considered in this work for two gases, argon and water. Important parameters of the model, such as the binding energy and the heat capacity as function of cluster size, are refined as compared to the previous work.[23] For argon, the present model was found to match theoretical dimer formation rate and equilirbium constant in the wide range of temperautres. In this case, a temperature-dependent inelastic collision number for monomer-cluster interactions was introduced. For water, two datasets were used, one based on quantum calculations of heat capacity and binding energy available in the literature, and the other based on the present molecular dynamics computations.

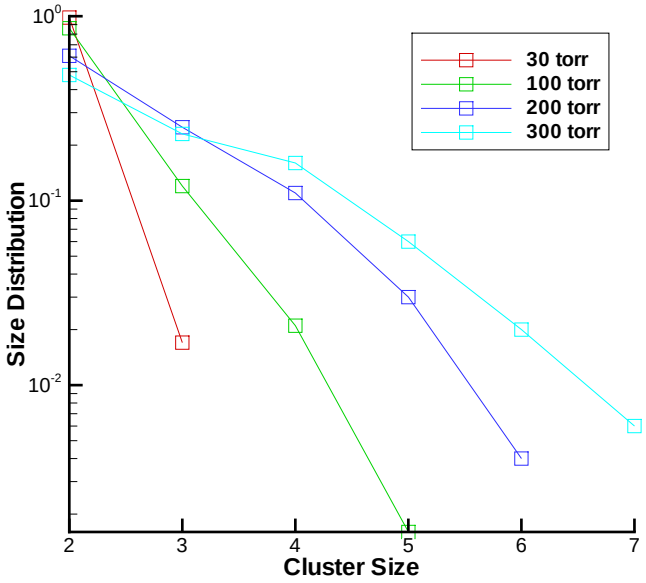

Figure 12. Terminal cluster size distribution function for different pressures at a stagnation temperature of 373 K.

For both datasets, the computed equilibrium constant as a function of temperature has lower slope than the available theoretical prediction. Comparison of water dimer formation in a plume expanding through a circular orifice, with experimental data shows good agreement at lower pressures and significantly lower numerical values for higher pressures. Further analysis is needed to clarify the reasons for such a difference.

VII. Acknowledgments

The authors are extremely thankful to Dr. Matthew Braunstein for his help with water binding energy analysis, and Dr. Y. Scribano for providing additional data for water dimer binding energy and heat capacity. The work was supported by the Air Force Office of Scientific Research.

References

[1]F. Abraham, Homogeneous Nucleation Theory: The Pretransition Theory of Vapor Condensation. New York: Academic Press, 1974.

[2]A. Zettlemoyer, Nucleation Phenomena. New York: Wiley, 1977.

[3]A. Itkin and E. Kolesnichenko, Microscopic Theory of Condensation in Gases and Plasma. Singapore: World Scientific, 1997.

[4]B. S. Lukyanchuk, W. Marine, S. I. Anisimov, and G. A. Simakina, "Condensation of vapor and nanoclusters formation within the vapor plume, produced by ns-laser ablation of Si, Ge and C," Proceedings of SPIE, vol. 3, no. 618, p. 434, 1999.

[5]H. Haberland, "Experimental methods," in Clusters of Atoms and Molecules, edited by H. Haberland (Springer, Berlin), p. 207, 1994.

[6]M. A. Ratner, "Kinetics of cluster growth in expanding rare-gas jet," Low Temp. Phys. Translated from Russian Journal Fiz. Nizk. Temp, 25, 367, 1999., vol. 25, p. 266, 1999.

[7]Y. P. Raizer, "Condensation of a cloud of vaporized matter expanding in vacuum," Soviet Physics JETP, vol. 37, p. 1229, 1959.

[8]J. Zhong, M. Zeifman, S. Gimelshein, and D. Levin, "Direct Simulation Monte Carlo Modeling of Homogenous Condensation in Supersonic Plumes," AIAA Journal, 2005, Vol. 43, No. 8, pp. 1784-1796.

[9]J. Zhong, D. A. Levin, and M. I. Zeifman, "Modeling of argon condensation in free jet expansions with the DSMC method," Proc. XXIV Int. Symp. on Rarefied Gas Dynamics, ed. M Capitelli, AIP Conference Proceedings, Vol. 762, New York, 2005, pp. 391-395.

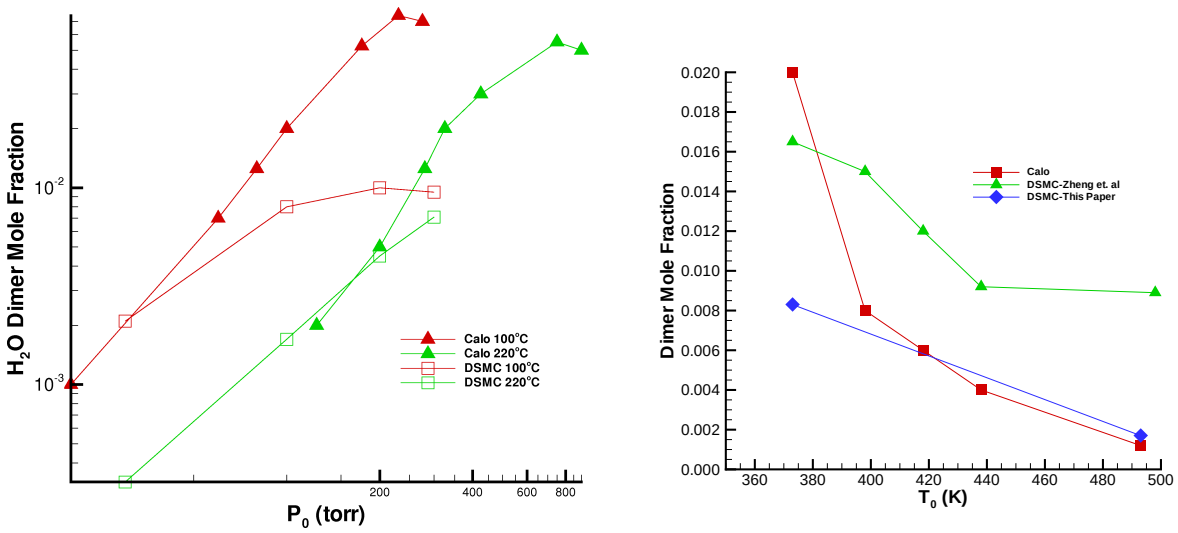

Figure 13. Comparison of terminal dimer mole fraction with experimental data[67] at different pressures (left) and numerical prediction[10] at 100 torr (right).

[10]J. Zhong, N. Moghe, Zh. Li, D. Levin, "A unimolecular evaporation model for simulating argon condensation flows in direct simulation Monte Carlo," Phys. Fluids, **21**, 2009, 036101.

[11]Ohkubo et al [Ohkubo, M. Kuwata, B. Lukyanchuk, and T. Yabe, "Numerical analysis of nanocluster formation within ns-laser ablation plume," Appl. Phys., vol. A 77, p. 271, 2003.

[12]G. A. Bird, Molecular Gas Dynamics and the Direct Simulation of Gas Flows. Oxford: Clarendon Press, 1994.

[13]H. Hettema and J. McFeaters, "The direct Monte Carlo method applied to the homogeneous nucleation problem," J. Chem. Phys., vol. 105, p. 2816, 1996.

[14]H. Mizuseki, Y. Jin, Y. Kawazoe, and L. T. Wille, "Growth processes of magnetic clusters studied by direct simulation Monte Carlo method," J. Appl. Phys., vol. 87, p. 6561, 2000.

[15]H. Mizuseki, K. Hongo, Y. Kawazoe, and L. Wille, "Multiscale simulation of cluster growth and deposition processes by hybrid model based on direct simulation Monte Carlo method," Comp. Mat. Sci, vol. 24, p. 88, 2002.

[16]J. Zhong, M. Zeifman, D. Levin, Kinetic model of condensation in a free expanding jet, J. Thermophysics and heat transfer, 2006, Vol. 20, No. 1, pp. 41-51.

[17]A. Gallagher-Rogers, J. Zhong, D.A. Levin, "Simulation of Homogeneous Ethanol Condensation in Supersonic Nozzle Flows Using DSMC," AIAA Paper 2007-4159.

[18]J. Zhong and D. Levin, "Development of a Kinetic Nucleation Model for a Free-Expanding Argon Condensation Flow," AIAA Journal, 2007, Vol. 45, No. 4, pp. 902-911,

[19]B. Briehl and H. Urbassek, "Monte Carlo simulation of growth and decay processes in a cluster aggregation source," J. Vac. Sci. Tech., A, Vol. 17, No. 1, p. 256, 1999.

[20]S. Gratiy, J. Zhong, D.A. Levin, "Numerical Simulation of Argon Condensation with a Full Kinetic Approach in a Free-Expanding Jet," AIAA Paper 2006-3598.

[21]Zh. Li, J. Zhong, D.A. Levin, B.J. Garrison, "Kinetic nucleation model for free expanding water condensation plume simulations," J. Chem. Phys., **130**, 2009, 174309.

[22]Li, Z., Zhong, J., Levin, D.A., and Garrison, B.J., "Development of Homogeneous Water Condensation Models Using Molecular Dynamics," *AIAA Journal*, Vol. 47, No. 5, 2009, pp. 1241-1251.

[23]R. Jansen, S. Gimelshein, M. Zeifman, I. Wysong, First-Principles Monte-Carlo Simulation of Homogeneous Condensation in Atomic and Molecular Plumes, AIAA Paper 2009-3745.

[24]R.D. Levine, Molecular reaction dynamics, Cambridge University Press, 2005.

[25]S.F. Gimelshein, M.S. Ivanov, "Simulation of Chemically Reacting Gas Flow Using Majorant Frequency Scheme of DSMC," Proc. XVII Intern. Symp. on Rarefied Gas Dynamics. Vancouver, Canada. 1994. Vol.159. pp. 218-233.

[26]D.L. Bunker, "Mechanisms of atomic recombination reactions," J. Chem. Physics, 1959, Vol. 32, No. 4, pp. 1001-1005.

[27]M.S. Ivanov and S.V. Rogasinsky, "Analysis of numerical techniques of the direct simulation Monte Carlo method in the rarefied gas dynamics," *Sov. J. Numer. Anal. Math. Modelling* **2** (6), 1988, pp. 453-465.

[28]G.A. Bird, "Monte-Carlo simulation in an engineering context," In *Rarefied Gas Dynamics,* ed. S Fisher, Progress in Astronautics and Aeronautics, 1981, vol. 74, pp. 239-255.

[29]models for internal energy exchange J. Zhong, M.I. Zeifman, D.A. Levin, Sensitivity of water condensation in a supersonic plume to the nucleation rate, J. Thermophysics and Heat Transfer, **20** (3), 2006, pp. 517-523.

[30]C. Borgnakke and P.S. Larsen, "Statistical collision model for Monte Carlo simulation of polyatomic gas mixture," J. Comp. Phys., 1975, Vol. 18, pp. 405-420.

[31]P.F. Zittel, D.E. Masturzo, "vibrational relaxation of H_2O from 295 K to 1020 K," J. Chem. Phys., **90** (2), 1989, pp. 977-989.

[32]N.E. Gimelshein, "Enhanced direct simulation Monte Carlo models for internal energy exchange and chemical reactions," M.S. Thesis, Penn State, 2002.

[33]C. Bobbert, S. Schutte, C. Steinbach, U. Buck, "Fragmentation and reliable size distributions of large ammonia and water clusters," Eur. Phys. J. D **19** pp. 183-192, 2002.

[34]J.F. Crifo, Water clusters in the coma of Comet Halley and their effect on the gas density, temperature, and velocity, ICARUS, **84**, 1990, pp. 414-446.

[35]M. Zeifman, B. J. Garrison, , and L. V. Zhigilei, "Combined molecular dynamics – direct simulation Monte Carlo computational simulation of laser ablation plume evolution," J. Appl. Phys., vol. 92, p. 2181, 2002.

[36]Y. Okada, Y. Hara, Calculation of the sticking probability of a water molecule to a water cluster, Earozoru Kenkyu, **22** (2), 2007, pp. 147-151.

[37]M. Braunstein, Private communication, 2009.

[38]S.S. Xantheas, C.J. Burnham, R.J. Harrison, "Development of transferable interaction models for water. II. Accurate energetics of the first few water clusters from first principles," J. Chem. Phys., **116**, 2002, pp. 1493-1499.

[39]K. Diri, E.M. Myshakin, K.D. Jordan, "On the Contribution of Vibrational Anharmonicity to the Binding Energies of Water Clusters," J. Phys. Chem., **109**, 2005, pp. 4005-4009.

[40]H.M. Lee, S.B. Suh, J.Y. Lee, P. Tarakeshwar, K.S. Kim, "Structures, energies, vibrational spectra, and electronic properties of mater monomer to decamer," J. Chem. Physics, vol. 112, no. 22, pp. 9759-9772.

[41]J.T. Su, X. Xu, W.A. Goddard III, "Accurate energies and structures for large water clusters using the X3LYP hybrid density functional," J. Phys. Chem. A, Vol. 108, pp. 10518-10526.

[42]L.L. Lohr, "Rotational energy dispersions for argon clusters," Molecular Physics, **85** (3), 1995, pp. 607-617.

[43]Y. Scribano, N. Goldman, R.J. Saykally, C. Leforestier, "Water dimers in the atmpsphere III: equilibrium constant from a flexible potential," J. Phys. Chem. A, **110** (16), 2006, pp. 5411-5419.

[44]P.A. frantsuzov, V.A. Mandelshtam, "Equilibrium properties of quantum water clusters by the variational Gaussian wavepacket method," J. Chem. Phys. **128**, 2008, 094304.

[45]S.A. Losev, S.O. Macheret, B.V. Potapkin, G.G. Chernyi, Physical and chemical processes and gas dynamics: cross sections and rate constants. Progress in Astronautics and Aeronautics, 196, AIAA, 2002.

[46]M.S. Ivanov, G.N. Markelov, S.F. Gimelshein, "Statistical simulation of the transition between regular and Mach reflection in steady flows," Computers and Mathematics with Applications, **35** (1-2), 1998, pp. 113-126.

[47]Tsai, C.J., and Jordan, K.D., "Monte Carlo Simulation of $(H_2O)_8$: Evidence for a Low-Energy S_4 Structure and Characterization of the Solid - Liquid Transition," *Journal of Chemical Physics*, Vol. 95, No. 5, 1991, pp. 3850-3853.

[48]Tsai, C.J., and Jordan, K.D., "Use of the Histogram and Jump-Walking Methods for Overcoming Slow Barrier Crossing Behavior in Monte Carlo Simulations: Applications to the Phase Transitions in the $(Ar)_{13}$ and $(H_2O)_8$ Clusters," *Journal of Chemical Physics*, Vol. 99, No. 9, 1993, pp. 6957-6970.

[49]Cao, J., and Berne, B.J., "Monte Carlo Methods for Accelerating Barrier Crossing: Anti-Force-Bias and Variable Step Algorithms," *Journal of Chemical Physics*, Vol. 92, No. 3, 1990, pp. 1980-1985.

[50]Frantz, D.D., Freeman, D.L., and Doll, J.D., "Reducing Quasi-Ergodic Behavior in Monte Carlo Simulations by J-walking: Applications to Atomic Clusters," *Journal of Chemical Physics*, Vol. 93, No. 4, 1990, pp. 2769-2784.

[51]Newman, M.E.J., and Barkema, G.T., *Monte Carlo Methods in Statistical Physics*, (Clarendon, Oxford, 1999).

[52]Jorgensen, W.L., "Revised TIPS for Simulations of Liquid Water and Aqueous Solutions," *Journal of Chemical Physics*, Vol. 77, No. 8, 1982, pp. 4156-4163.

[53]Jorgensen, W.L., and Madura, J.D., "Temperature and Size Dependence for Monte Carlo Simulations of TIP4P Water," *Molecular Physics Journal*, Vol. 56, No. 6, 1985, pp. 1381-1392.

[54]Guvenc, Z.B., and Anderson, M.A., "A Molecular Dynamics Study of Small Water Clusters Comparing Two Flexible Models for Water," *Zeitschrift fur Physik D*, Vol. 36, 1996, pp. 171-183.

[55]Pedulla, J.M., and Jordan, K.D., "Melting Behavior of the $(H_2O)_6$ and $(H_2O)_8$ Clusters," *Chemical Physics*, Vol. 239, 1998, pp. 593-601.

[56]Carignano, M.A., "Monte Carlo Simulations of Small Water Clusters: Microcanonical vs Canonical Ensemble," *Chemical Physics Letters*, Vol. 361, 2002, pp. 291-297.

[57]Mahoney, M.W., and Jorgensen, W.L., "A Five-Site Model for Liquid Water and the Reproduction of the Density Anomaly by Rigid, Nonpolarizable Potential Functions," *Journal of Chemical Physics*, Vol. 112, No. 20, 2000, pp. 8910-8922.

[58]Shin, S., Son, W.J., and Jang, S., "Quamtum Phase Transition of Water Clusters: Molecular Dynamics Simulations with a Model Potential," *Journal of Molecular Structure*, Vol. 673, 2004, pp. 109-113.

[59]Lobaugh, J., and Voth, G.A., "A Quantum Model for Water: Equilibrium and Dynamical Properties," *Journal of Chemical Physics*, Vol. 106, No. 6, 1997, pp. 2400-2410.

[60]Berendsen, H.J.C., Psotma, J.P.M., van Gunsteren, W.F., and Hermans, J., "Interaction Models for Water in Relation to Protein Hydration", *Intermolecular Forces*, edited by B. Pullman, D. Reidel Publishing Co., Dordrecht, The Netherlands, 1981, p. 331-342.

[61]Schenter, G.K., Kathmann, S.M., and Garrett, B.C., "Dynamical Benchmarks of the Nucleation Kinetics of Water," *Journal of Chemical Physics*, Vol. 116, No. 10, 2002, pp. 4275-4280.

[62]R. Kalus, "Formation of argon dimers in ternary monomer collisions," J. Chem. Phys., **109** (19), 1998, pp. 8289-8294.

[63]P.S. Dardi, J.S. Dahler, "Equilibrium constants for the formation of van der Waals dimers: Calculations, for Ar-Ar and Mg-Mg," J. Chem. Phys., **93** (5), 1990, pp. 3562-3572.

[64]R.E. Leckenby, E.J. Robbins, "The observation of double molecules in gases," Proc. Royal Soc. London, Series A, 1966, pp. 389-412.

[65]D.E. Stogryn, J.O. Hirschfelder, "Contribution of bound, metastable, and free molecules to the second virial coefficient and some properties of double molecules," J. Chem. Phys., **31** (6), 1959, pp. 1531-1544.

[66]Y. Scribano, Private Communication, 2009.
[67]J.M. Calo, "Dimer formation in supersonic water vapor molecular beams," J. Chem. Phys., **62** (12), 1975, pp. 4904-4910.